

# PALM KERNEL SHELL BIOCHAR PRODUCTION, CHARACTERISTICS AND CARBON SEQUESTRATION POTENTIAL

SIENG-HUAT KONG\*; SOH KHEANG LOH\*\*; ROBERT THOMAS BACHMANN‡;  
HARYATI ZAINAL\*\* and KAH YEIN CHEONG\*

## ABSTRACT

Properties of palm kernel shell (PKS) biochar were studied to identify its potential for soil amendment and carbon sequestration. In this study, slow pyrolysis of PKS was conducted using the Biochar Experimenters Kit at final temperatures 400°C - 600°C and holding times 30 - 90 min with a heating rate of  $7.3 \pm 0.6^\circ\text{C min}^{-1}$ . Samples were characterised using CHNS/O analyser, Brunauer-Emmet-Teller (BET), leaching column for cation exchange capacity (CEC), energy dispersive X-ray (EDX) and Fourier transform infrared (FTIR) spectrometers. The C content increased from 46 wt.% to 73 wt.% after pyrolysis, while hydrogen (H) and oxygen (O) contents decreased due to dehydration, decarboxylation and demethanation. The molar H/C and O/C ratios of PKS biochar ranged from 0.32-0.54 and 0.08-0.21, respectively, suggesting high stability in soil. PKS biochar at 500°C (90 min) exhibited the greatest carbon sequestration potential of  $0.63 \text{ kgCO}_2/\text{kg}_{\text{PKS}}$ . The pH was between 9.3 to 12.0, while CEC increased from 3.00 to 4.44  $\text{cmol kg}^{-1}$  only for biochar at 400°C (60 min). The BET surface area and total pore volume increased from  $106 \text{ m}^2 \text{ g}^{-1}$  and  $0.01 \text{ cm}^3 \text{ g}^{-1}$  (raw) to  $329 \text{ m}^2 \text{ g}^{-1}$  and  $0.31 \text{ cm}^3 \text{ g}^{-1}$  (biochar) at 600°C (60 min) whereas water holding capacity increased from  $2.23 \text{ g(H}_2\text{O)/10 g}$  to  $6.21 \text{ g(H}_2\text{O)/10 g}$  at 500°C (30 min), respectively. Plant nutrients were retained in PKS biochar (400°C and 500°C). PKS biochar can potentially sequester carbon and improve nutrient and water retention in acidic low-fertility soils.

**Keywords:** biochar, palm kernel shell, pyrolysis, carbon sequestration, soil application.

**Date received:** 1 April 2019; **Sent for revision:** 1 April 2019; **Received in final form:** 31 July 2019; **Accepted:** 1 August 2019.

## INTRODUCTION

To date, conversion of oil palm biomass into biochar, a carbon-rich product obtained from thermal

decomposition of biomass under limited or no supply of oxygen, has drawn considerable attention from the scientific community for two reasons; to enhance and diversify the abundantly available biomass residues and to identify its potential in mitigating greenhouse gas (GHG) emissions via soil amendment. However, the long-term effects of biochar on carbon sequestration, soil fertility and environmental remediation are highly dependent on its physico-chemical properties (Spokas *et al.*, 2009; Ahmad *et al.*, 2014).

The specific properties of biochar materials are influenced by the feedstock and thermo-chemical process used which in turn change the soil nutrients, water and carbon availability (Karaosmanoglu *et al.*,

\* School of Foundation Studies,  
University College of Technology Sarawak,  
Lot 868 Persiaran Brooke, 96000 Sibul,  
Sarawak, Malaysia.

\*\* Malaysian Palm Oil Board, 6 Persiaran Institusi,  
Bandar Baru Bangi,  
43000 Kajang, Selangor, Malaysia.  
E-mail: lohsk@mpob.gov.my

‡ Universiti Kuala Lumpur (UniKL),  
Malaysian Institute of Chemical and Bioengineering Technology  
(MICET), Lot 1988 Kawasan Perindustrian, Bandar Vendor,  
Taboh Naning, 78000 Alor Gajah, Melaka, Malaysia.

2000). Biochar application to various types of soil has been reported causing either neutral, beneficial or in isolated cases detrimental effects on plants growth (Kong *et al.*, 2014; Galinato *et al.*, 2011; Liu *et al.*, 2013). Among the reported benefits, the crucial ones include an increased water holding capacity, improved nutrient retention and availability, and a reduced nutrient loss from leaching (Karhu *et al.*, 2011; Mollinedo *et al.*, 2015). Equally important, biochar can store C for centuries due to its strong resistance to biological decomposition (Preston and Schmidt, 2006; Liang *et al.*, 2008; Van Zwieten *et al.*, 2009). A weighted meta-analysis of 103 studies revealed that biochar soil amendment induced a greater crop response in pot experiments (9.0% on average) than in field (11.0%), in acid (30%, pH < 5.0) than in quasi-neutral soils (< 15%, pH > 5.0), in sandy textured (29.3%) and clay (15.7%) than in loam and silt (6.8%) soils, in dry land crops (10.6%) than for paddy rice (5.6%), while acidic biochars had an overall negative effect on crop productivity (Liu *et al.*, 2013). From their analysis, the authors suggested that the observed crop response was mainly due to a combination of liming and aggregating/moistening effect of biochar soil amendment.

Previous studies have shown that the composition and surface chemistry of biochars are highly uncertain and subject to operating conditions (Usman *et al.*, 2015; Zhang *et al.*, 2015; Rafiq *et al.*, 2016). In particular, an increase in the process temperature not only improves the biochar adsorption properties such as surface area and porosity, but also increases the pH value for liming effects (Jindo *et al.*, 2014; Gai *et al.*, 2014). It is important to note that the employed pyrolysis temperature could volatilise some elements such as N and S, but C, P, Mg and Ca would be partially or fully retained and concentrated in the resulting biochar (Bridle and Pritchard, 2004). Compared to pyrolysis temperature, holding time has a relatively minor effect on the properties changes especially for smaller particles (Zhang *et al.*, 2015; Li *et al.*, 2015; Shaaban *et al.*, 2014).

Solid oil palm biomass residues are generated throughout the year in palm oil mills and oil palm plantations. One of them, palm kernel shell (PKS), has the highest commercial utilisation value. PKS was chosen as a feedstock for this study due to its high lignin content (47.3%-50.7%) which is essential for thermal conversion into biochar (Choi *et al.*, 2015; Kataki *et al.*, 2015; Loh, 2017). Its particle size of about 1.5 cm is suitable to be loaded directly into any design of pyrolysis reactor without further downsizing and pre-treatment.

Various types of PKS biochar were produced under different process parameters and experimental set-up. Previously, PKS torrefied at 240°C-280°C and 30, 60 and 90 min has shown a greater temperature effect than holding time in the biomass-to-biochar

conversion process (Jaafar and Ahmad, 2011). PKS gasified at high temperature (650°C-800°C) has shown ~81% carbon content which is convincing as a soil amendment material for carbon sequestration (Mahmood *et al.*, 2015). PKS pyrolysed in a pilot-scale fixed-bed reactor under allothermal conditions was found to be a potentially suitable carbon sink as was evidenced by the high carbon content (up to 74 wt.%) and stability (in terms of volatile matter *vs.* fixed carbon, H/C and O/C) (Haryati *et al.*, 2018). The surface area of the most recently studied microwave-pyrolysed PKS increases with increasing temperature from 300°C to 700°C in a porcelain reactor, while H/C and O/C ratios decrease showing greater stability of the biochar in storing carbon (Kong *et al.*, 2019). These studies, however, have only managed to show a general trend on biochar soil amendment properties affected by temperature and holding time, but lacking in detailing how these two process parameters might impart on the char's carbon sequestration potential. This study aims to investigate the influence of pyrolysis temperature and holding time on the physico-chemical characteristics of PKS. The resulting PKS biochar's suitability as a carbon sink and for soil amendment was assessed by estimating its carbon sequestration potential (CSP).

## MATERIALS AND METHODS

### Sample Preparation

The PKS was collected in bulk from Sime Darby Palm Oil Mill located in Labu, Negeri Sembilan, Malaysia. The PKS was spread and air-dried at ambient temperature under a covered area for a week. Before being filled into the biomass hopper for pyrolysis, the PKS was manually screened for pebbles and other foreign objects.

### Production of Biochar

Pyrolysis of PKS was carried out using the Biochar Experimenters Kit (BEK) from All Power Labs, California (USA) according to Haryati *et al.* (2018). Two series of experiments were conducted focusing on the effects of final pyrolysis temperature and holding time on the physico-chemical properties of biochar produced. The first series of experiments performed at 400°C, 500°C and 600°C for a fixed holding time of 60 min produced biochar coded as BC400 (60 min), BC500 (60 min) and BC600 (60 min). The biochar from the second series of experiments at three different pyrolysis holding times (30, 60 and 90 min) at a fixed temperature of 500°C were coded BC500 (30 min), BC500 (60 min) and BC500 (90 min). The pyrolysis temperature increased gradually to the desired value (designated as final

pyrolysis temperature), and then was held for the required period (designated as holding time). A thermocouple (RS Pro Type-K) with data logger on top of the reactor was used to measure the temperature inside the reactor (Haryati *et al.*, 2018).

### Characterisation of PKS and Biochar

Both the feedstock and PKS biochar were ground for 90 s using an automatic electric grinder (Dickson DFY-300). The samples were then mixed and homogenised for further analysis. All samples were kept air tight inside plastic sample bottles and stored in a cool and dry cabinet. The total carbon (C), hydrogen (H), nitrogen (N) and sulphur (S) content were measured by a CHNS analyser (Leco CHNS 628 Series) in accordance with ASTM D 5373. The oxygen (O) content was calculated by subtracting the weight percentage between all the elements plus ash from the total of 100%. Prior to the analysis, the samples were dried in an oven at 105°C for 15 hr. The molar ratios (O/C and H/C) were calculated based on the measured C, H and O contents. Energy dispersive X-ray (EDX) spectroscopy was performed at an accelerating voltage of 20 kV using an Oxford INCA X-max detector. The uncoated sample was mounted on a scanning electron microscopy (SEM) stub using double-sided carbon tape and investigated for elemental composition by conducting 2D analyses of six particles per biochar type.

The pH values of all samples were measured using a calibrated pH meter (Eutech Instruments, pH tutor) at 1:10 (w/v) sample to deionised water ratio after the mixture of solution was shaken at 100 rpm and allowed to reach equilibrium for 2 hr (EPA Method 9045D). The electrode was directly dipped into the solution and the reading was recorded as pH of the sample. The cation exchange capacity (CEC) was determined to estimate the biochar ability to attract, retain and exchange cations based on method proposed by Soda *et al.* (2006) using 1 M ammonium acetate (NH<sub>4</sub>OAc) at pH 7. The total amount of NH<sub>4</sub><sup>+</sup> retained by the biochar (after washing and leaching) was determined via titration (Loh *et al.*, 2015) and regarded as an estimate of the CEC.

The chemical functional groups and bonds of the biochar were identified with a Fourier transform infrared (FTIR) spectrometer (Perkin-Elmer Spectrum 100) via KBr disc method. The biochar sample was first mixed with oven-dried KBr, followed by pressurising using a hydraulic press at 8 to 10 t of pressure for 3 to 5 min before subjecting to FTIR analysis. The FTIR spectra were recorded in the range of 4000-500 cm<sup>-1</sup> at a resolution of 4 cm<sup>-1</sup> with 16 scans.

The Brunauer-Emmet-Teller (BET) surface area and total pore volume of the PKS and PKS biochar were measured via nitrogen adsorption-desorption

isotherms at -196°C using an accelerated surface area and porosimetry system (ASAP 2010, Micromeritics USA). The BET surface area was calculated in m<sup>2</sup> g<sup>-1</sup> using the adsorption data in the relative pressure range from 0.05 to 0.25. The total pore volume was determined by converting the amount of nitrogen gas adsorbed, in cm<sup>3</sup> g<sup>-1</sup> at S.T.P, at relative pressure of 0.98 to the volume of liquid adsorbate. The water holding capacity was calculated as g g<sup>-1</sup> water held in 10 g of biochar sample on dry weight basis (d.w.b.). Biochar samples were dried at 105°C for 15 hr and placed inside the funnels containing filter paper. Deionised water was dripped into the funnels at a fixed rate for 15 min. After the biochar samples were completely immersed in water, excess water was drained off through the bottom of the funnel (Saarnio *et al.*, 2013). Prior to the experiments, a blank run (without biochar sample) was conducted in order to find out the weight of the wet filter paper inside the funnel.

### Carbon Sequestration Potential (CSP)

The CSP of PKS biochar was estimated on a one-hundred-year basis. Equation (1) derived from Budai *et al.* (2013) was used to predict the CSP (kgCO<sub>2</sub>/kg<sub>biomass</sub>).

$$CSP = \frac{BC_{+100}}{100\%} \times Y_c \times \frac{44}{12} \quad \text{Equation (1)}$$

where BC<sub>+100</sub> is the organic C biochar projected to remain in the soil after 100 years (d.w.b.) [wt.%], and Y<sub>c</sub> is the organic C yield (d.w.b.) [g<sub>organic carbon</sub>/g<sub>biomass</sub>].

Budai *et al.* (2013) reported the BC<sub>+100</sub> parameter to be a linear function of the H/C<sub>org</sub> ratio [Equation (2)] valid for H/C<sub>org</sub> ratios ≤ 0.7. In Equation (2), C<sub>org</sub> is the organic C content.

$$BC_{+100} (\%) = -74.3 \times \frac{H}{C_{org}} + 110.2 \quad \text{Equation (2)}$$

Since the inorganic C fraction in low-ash biochars is negligible (Enders *et al.*, 2012), the C<sub>org</sub> of PKS biochars was assumed to be equivalent to the total carbon as determined by ultimate analysis.

## RESULTS AND DISCUSSION

Several parameters need to be considered when conducting pyrolysis experiments. One concern is temperature range of the reactor used to produce biochar. The temperature range depends not only on the components used (*e.g.* stainless steel *vs.* mild

steel) but also health and safety concerns. Another aspect is related to the feedstock properties. From previous thermogravimetric analysis (TGA) studies (Ma *et al.*, 2017; 2019), it is known that hemicellulose and cellulose decompose at temperatures between  $\sim 250^{\circ}\text{C}$  and  $\sim 400^{\circ}\text{C}$  while lignin decomposes over a wider temperature range. In order to ensure that the least stable biomass components (hemicellulose and cellulose) are decomposed,  $400^{\circ}\text{C}$  was selected as the lowest temperature while  $600^{\circ}\text{C}$  was the upper limit of the BEK reactor at which we could safely operate. Thus,  $500^{\circ}\text{C}$  was selected as the centre point to further investigate the effect of holding time (on biochar-relevant physico-chemical characteristics and CSP).

### Elemental Composition

The elemental composition of the raw and pyrolysed PKS (d.w.b.) are presented in Figure 1. The C content increased while that of H, O and S decreased with increasing temperature. The high content of C ( $71.1 \pm 0.1$  wt.% to  $73.1 \pm 0.3$  wt.%) showed a  $> 50$  wt.% biomass-to-biochar conversion rate by BEK at  $400^{\circ}\text{C}$  suggesting that the conversion of the main constituents, *i.e.* hemicellulose, cellulose and lignin to volatiles and aromatic carbon is almost complete at 60 min holding time.

A decline in H (25%) and O (42%) content with higher pyrolysis temperatures was observed (Figure 1) which could be due to the breaking of oxygen-containing functional groups (such as carboxyl, carbonyl and methoxyl) from their polymeric backbone (Ma *et al.*, 2017) as well as formation of highly carbonaceous, aromatic compounds (Imam

and Capareda, 2012; Demirbas, 2004). As for N and S, their presence in the raw PKS itself were already very low ( $< 1$  wt.%) in the case of N or below the detection limit for S (Haryati *et al.*, 2018), decreasing further in the produced biochar. Similar findings have been reported by Ma *et al.* (2017) who pyrolysed PKS in a quartz tube furnace at  $250^{\circ}\text{C}$  to  $750^{\circ}\text{C}$  for 1 hr.

The effect of holding time on the PKS biochar elemental contents (C, H and O) was less pronounced and revealed that the H/C ratio decreased from 0.51 for BC500 (30 min) to 0.32 for BC500 (90 min) (Figure 2).

In Haryati *et al.* (2018), we anticipated that PKS biochar will inherit micro- and macro-nutrients beneficial as a feed material and for soil amendment. In this study, in addition to the overall elemental content of PKS and its pyrolysed form, EDX was deployed to identify the elemental composition of BC400, BC500 and BC600 surfaces (Figure 3). C and O were always detected and the most abundant elements. The most frequent minerals present were Ca, K and Si followed by Al. Iron (Fe) was occasionally observed on BC400 (60 min), while Mg was sometimes found on BC500 (60 min). Phosphorus (P) started to appear in BC500 (60 min). S, N, Cl and Na were always below the detection limit ( $\sim 0.1$  wt.%). C increased from 71.6 wt.%, BC400 (60 min) to 87.2 wt.%, BC500 (60 min) ( $p = 0.167$ ) while O decreased from 20.2 wt.%, BC400 (60 min) to 8.3 wt.%, BC500 (60 min) ( $p = 0.059$ ) which agrees with the trend reported in Figure 1.

Ca content increased by a factor of 5 from 0.6 wt.% (BC400, 60 min) to 2.8 wt.% (BC500, 60 min) ( $p = 0.068$ ), while K almost doubled from 0.29 wt.%

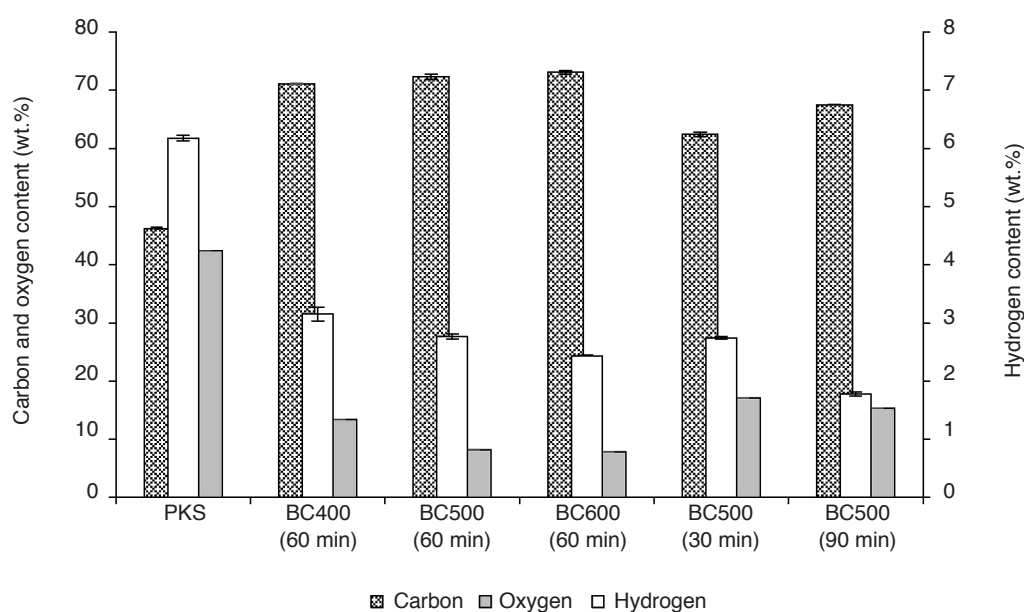


Figure 1. Elemental content of original and pyrolysed palm kernel shell (PKS) (d.w.b.). Oxygen content was calculated by percentage difference. Sulphur content was below detection limit.

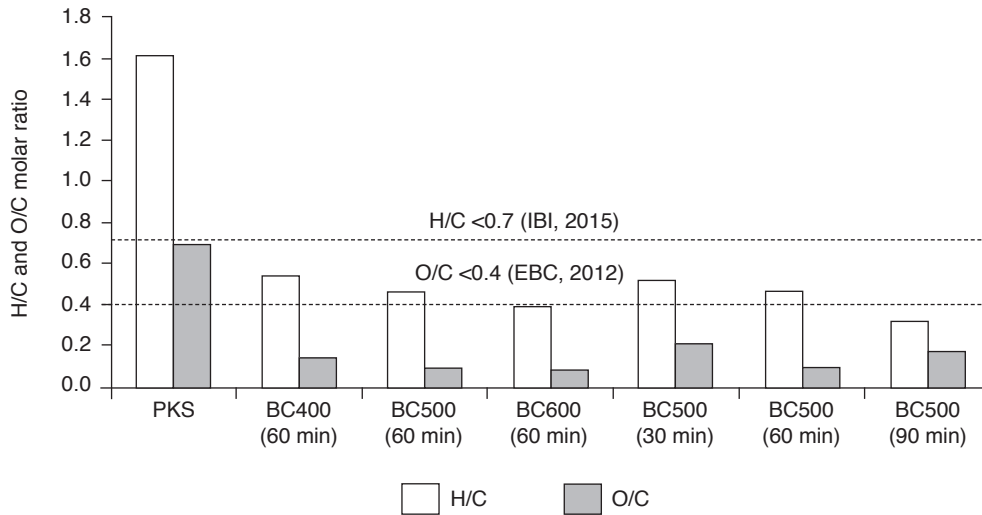


Figure 2. Atomic H/C and O/C ratios of original and pyrolysed palm kernel shell (PKS).

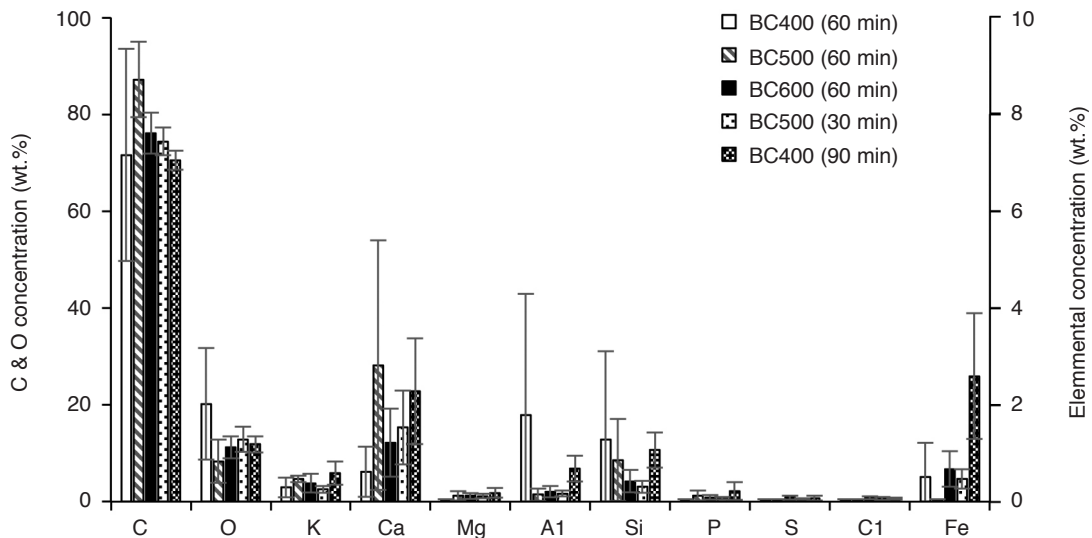


Figure 3. Elemental composition of palm kernel shell biochar pyrolysed at 400°C (BC400), 500°C (BC500) and 600°C (BC600) and holding times of 30-90 min (n = 6).

(BC400, 60 min) to 0.59 wt.% (BC500, 90 min) ( $p = 0.022$ ). Alkali and alkaline earth metals K, Ca and Mg are valuable macronutrients for plants and appeared to be retained in BC400 (60 min) and BC500 (60 min). This agrees with Liu *et al.* (2017) who reviewed the fate of organic and inorganic elements during pyrolysis. The authors reported that Ca and Mg are more likely retained in the biochar phase than Na and K, while temperatures  $>600^{\circ}\text{C}$ , high heating as well as gas flow rates promote the release of these metals from biomass during pyrolysis. Since pyrolysis temperature studied was between  $400^{\circ}\text{C}$  and  $600^{\circ}\text{C}$  plus heating rate was slow with no forced gas flow through the BEK reactor, it suggests that alkali and alkaline earth metals were mainly

retained within the PKS biochars at investigated conditions.

S is taken up by plants as sulphate, transported to stems and leaves, reduced to sulphide and incorporated into amino acid cysteine. This process occurs continuously in plants, hence, both organic and inorganic species are present (Liu *et al.*, 2017). During pyrolysis the organic S can be released as  $\text{SO}_2$ ,  $\text{H}_2\text{S}$  and metal sulphides at  $400^{\circ}\text{C}$  while inorganic sulphate is highly stable and remains with biochar. Kim *et al.* (2014) pyrolysed PKS in a fluidised bed reactor at  $485^{\circ}\text{C}$  and found 0.18% S in the bio-oil. In our work, S content was often close to the detection limit (BC400 and BC500) and appeared to increase with pyrolysis temperature

[(0.8 ± 0.4 wt.% for BC600 (60 min)] and holding time. This finding, combined with the fact that PKS is dominated by hemicellulose, cellulose and lignin (Kong *et al.*, 2014), suggest that S content in PKS biochar was primarily of inorganic origin.

N is a major element required by plants to promote the formation of shoots and roots as well as synthesise proteins. During pyrolysis release of N in the form of HCN and NH<sub>3</sub> can start at temperatures as low as 200°C. Decomposition and release is influenced by presence of hemicellulose (inhibits formation of NH<sub>3</sub>), and lignin (promotes NH<sub>3</sub> formation), heating rate and presence of inorganic elements (Liu *et al.*, 2017). Kim *et al.* (2014) reported a 6.65 wt.% N content in pyrolytic bio-oil from PKS which confirms the release of N from PKS during pyrolysis. The lack of proteins in PKS coupled with the volatilisation of N during pyrolysis explains why this element was not detected in PKS biochars produced in this study. The absence of N in both biochars agrees with the ultimate analysis.

Cl is typically found in stems and leaves of plants (Liu *et al.*, 2017). It is associated with inorganic species such as K (sylvite) and organics able to volatilise in two stages as HCl at <500°C and metal chlorides at >700°C during pyrolysis (Liu *et al.*, 2017). Cl content followed a similar trend to S content suggesting that it was associated with K to form sylvite. This is further supported by Clemente *et al.* (2018) who investigated inorganics in various biochars using XRD, SEM-EDX and principal component analysis. Principal component analysis was able to differentiate the EDX spectra into four main groups: (i) Ca, (ii) Fe, (iii) Al, Si and (iv) Cl, K, Mg, Na, P and S. Based on XRD these elements were also components of mineral phases such as Ca in calcite; Fe in magnetic Fe oxide; Si in quartz; K, Na, Ca, Al and Si in feldspar; and K and Cl in sylvite. However, further in-depth studies should be carried out to verify the mineral phases present in PKS biochar.

Overall, PKS biochar exhibited some essential nutrients which can potentially be used as a supplement to plant/animal growth.

### Biochar Stability and Carbon Sequestration Potential Assessment

As one of the roles of biochar is to store carbon, it is the C yield and H/C ratio that is more significant rather than the biochar yield in order to project the biochar effectiveness in CSP (Masek *et al.*, 2013; Enders *et al.*, 2012).

Our study showed that increasing pyrolysis temperature led to lower H/C and O/C ratios as the abundance of aromatic C increased relative to H and O due to dehydration and removal of O-H functional groups (Domingues *et al.*, 2017; Spokas, 2010; Krull *et al.*, 2009). The H/C and O/C

ratios of PKS biochar were 0.32-0.54 and 0.08-0.21, respectively (Figure 2), indicating high stability of the biochar due to an increased aromaticity (Bridgeman *et al.*, 2008) causing higher recalcitrance of C. Biochars with low H/C and O/C ratios are graphite-like materials or charcoal which are highly stable compared to their original biomass feedstock having higher H/C and O/C ratios (EBC, 2012; IBI, 2015). Based on experimental data reported by Ma *et al.* (2019), the molar O/C ratios of commercial microcrystalline cellulose, xylan and Klason lignin from PKS decrease from 0.95 to 0.17, 0.99 to 0.17 and 0.44 to 0.293, respectively, when heated to 450°C. This equates to a 5.4-, 5.6- and 1.5-fold decrease. TGA and solid state <sup>13</sup>C NMR demonstrated that all three biomass components have undergone profound structural changes with the obtained carbonised product dominated by the aromatic, highly stable aryl carbon. Considering that the O/C ratio of PKS in this study decreased at least 4.9-fold when pyrolysed at 400°C for 60 min, it can be expected with confidence without TGA that the PKS biochar is stable and less prone to degradation.

Our previous study (Haryati *et al.*, 2018) revealed higher H/C<sub>org</sub> values of 0.52 to 0.97. In this study, all H/C<sub>org</sub> values were < 0.7 which allowed us to proceed with the BC<sub>+100</sub> calculation using Equation (2). The BC<sub>+100</sub> values ranged from 70% for BC400 (60 min) to 86% for BC500 (90 min). The lowest corresponding CSP was estimated to be 0.49 kgCO<sub>2</sub>/kg<sub>PKS</sub> for BC500 (30 min) and greatest for BC500 (90 min) (0.63 kgCO<sub>2</sub>/kg<sub>PKS</sub>). From a CSP perspective, it is therefore recommended to pyrolyse PKS at 500°C for 90 min in order to immobilise the greatest amount of CO<sub>2</sub>. However, the operation of the BEK itself also consumes energy which comes with a CO<sub>2</sub> penalty. A life cycle analysis should therefore be carried out to quantify the CO<sub>2</sub> emissions as a function of pyrolysis temperature and holding time.

### Physico-chemical Properties

Raw PKS, a near-neutral pH material, was transformed to an alkaline biochar upon pyrolysis (pH 9.3 to 12.0). The pH increased sharply by up to 5.0 pH units from 7.0 to 9.3 at 400°C, 10.4 at 500°C and 12.0 at 600°C, in the order of BC600 (60 min) > BC500 (60 min) > BC 500 (30 min and 90 min) > BC400 (60 min), mainly due to enriched alkali species present in the inorganic ashes (Jindo *et al.*, 2014; Yuan *et al.*, 2011). The pH values and ash contents of biochars were positively correlated (Figure 3), justifying the present minerals as the main contributor to the alkalinity of PKS biochar (Zheng *et al.*, 2013). In general, all biochars pyrolysed in this study showed pH values >8.0. The higher pH range indicates a higher liming potential of the resulting PKS biochar which is desirable for acidic soils suffering from aluminum

toxicity and low P availability (Manickam *et al.*, 2015).

The CEC of PKS biochar decreased with an increase in pyrolysis temperature, in the order of BC400 (60 min) > BC500 (60 min) > BC500 (30 min) > BC500 (90 min) > BC600 (60 min). At initial biomass decomposition (400°C), many oxygenated compounds were formed. The resulting CEC was thus higher than that of raw PKS. However, as temperature increased further, the cellulose and lignin experienced a more severe thermal degradation (500°C and 600°C), releasing those formed oxygenated functional groups, *e.g.* carbonyl, and aromatisation took place. Negatively-charged groups on biochar surfaces were much reduced (Uttran *et al.*, 2018) causing lesser active sites for cation exchange. As shown in *Figure 4*, the CEC ( $4.44 \pm 0.31 \text{ cmol kg}^{-1}$ ) at 400°C dropped to  $2.34 \pm 0.06$  and  $1.01 \pm 0.15 \text{ cmol kg}^{-1}$  at 500°C and 600°C, respectively. Similar trend was observed by Gaskin *et al.* (2007). As temperature increased further, most of the carbonyl groups responsible for negative charges were lost, as supported by the disappearance of the FTIR bands at 1200-1300  $\text{cm}^{-1}$  attributed to C-O and O-H phenolic and 1500-1600  $\text{cm}^{-1}$  for conjugated C=C and C=O cyclic structure (*Figure 5*). In short, the removal of oxygen-containing functional groups from the cellulose, hemicellulose and lignin of PKS occurring at higher pyrolysis temperatures had caused loss of biochar surface capability in exchanging cations. However, as biochar CEC is mainly regulated by the biomass rather than by pyrolysis temperature (Domingues *et al.*, 2017), the fact that the PKS biochar showed low CEC means PKS constitutes very limited organic functional groups.

Similar to the trend of PKS biochar elemental contents at 500°C *vs.* holding time, the BC500 (60 min) hold the optimum alkalinity and CEC. At longer heating time (BC500, 90 min), volatilisation of C, O, and H compounds increased leading to more severe decomposition of surface functional group, and thus a decreased negative surface charge (Shaaban *et al.*, 2014).

### Functional Group Characteristics

The FTIR spectra (*Figure 5*) relate the production of PKS biochar as a function of pyrolysis temperature and holding time. Overall, *Figure 5* demonstrates a broad similarity amongst the produced PKS biochars even at downward shift of the entire band positions. These biochars showed distinctive bands different from its original form: 3858  $\text{cm}^{-1}$ -3737  $\text{cm}^{-1}$ , inter- and intramolecular hydrogen bonded O-H; 3406  $\text{cm}^{-1}$ , hydrogen-bonded O-H stretching; 2500-2336  $\text{cm}^{-1}$  S-H/acid O-H stretching; 1699  $\text{cm}^{-1}$ , carbonyl ester C=O stretching; 1424  $\text{cm}^{-1}$ ,  $\equiv\text{C-H}$  bend; 1214  $\text{cm}^{-1}$  and 1055  $\text{cm}^{-1}$ ; phenolic and alkoxy C-O stretching vibrations (Uttran *et al.*, 2018). The broad absorption bands at about 3400  $\text{cm}^{-1}$  exhibited by PKS biochar corresponded to a sharp decreased intensity of the -OH stretching of cellulose and hemicellulose which had decomposed. The bands in this region for BC500 (30 and 60 min) and BC400 (60 min) were more intense probably due to a larger proportion of the retained oxygenated functional groups at less severe pyrolysis conditions. As the conditions elevated, as in BC500 (90 min) and BC600 (60 min), the bands nearly disappeared due to degradation and dehydration (volatilisation) of cellulosic and

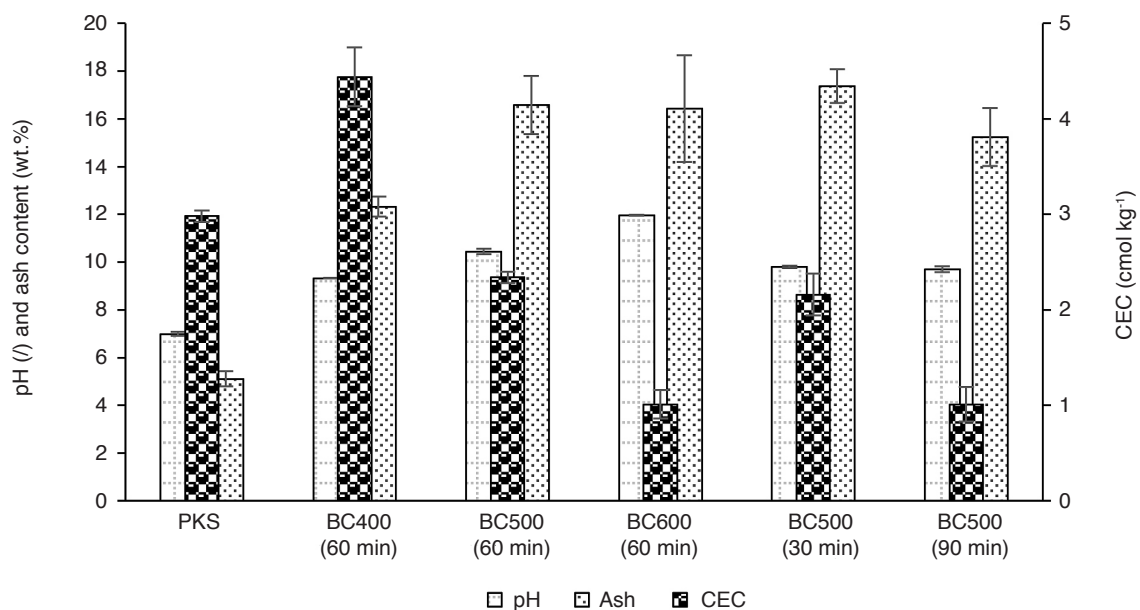


Figure 4. The pH, ash content and cation exchange capacity (CEC) of original and pyrolysed palm kernel shell (PKS).

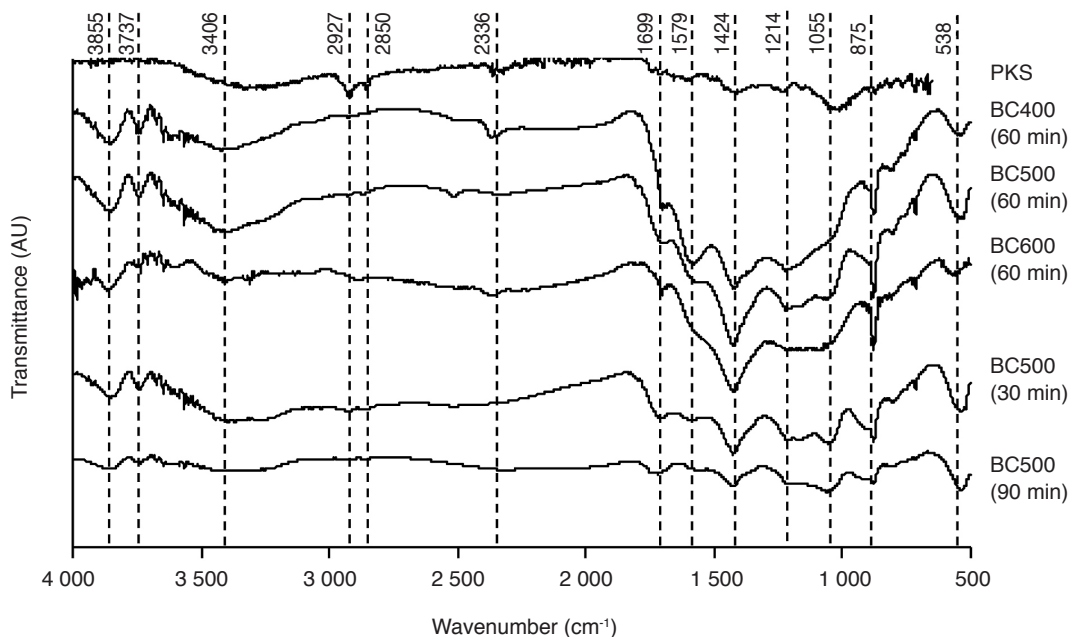


Figure 5. Spectral change with palm kernel shell (PKS) biochar formation temperatures and holding times.

ligneous components. Similarly, the two bands at 2927–2850  $\text{cm}^{-1}$  representing aliphatic C-H and O=C-H stretching of cellulose and hemicellulose had diminished entirely showing decompositions of these components during PKS pyrolysis.

The disappearance of aliphatic C-H stretching (2920–3000  $\text{cm}^{-1}$ ) and appearance of intense bands at 1500–1600  $\text{cm}^{-1}$  (aromatic C=C stretching), 1380–1450  $\text{cm}^{-1}$  (=C-H<sub>2</sub> bending) and between 875  $\text{cm}^{-1}$  (aromatic C-H bending) and 750  $\text{cm}^{-1}$  (aromatic CH out-of-plane) showed an increasing degree of condensation and aromatisation of the PKS biochar organic compounds (Domingues *et al.*, 2017; Brewer, 2012). The presence of aromatic

C=C in PKS biochar is indicative of a dominating delocalised conjugated non-fossil-based covalent bond providing extra stability in soils over time, hence better carbon storage/sequestration in long run (Abdulrazzaq *et al.*, 2014). Table 1 compares and summarises the characteristics FTIR bands of PKS biochars and raw PKS.

#### Surface Area and Pore Properties

The BET surface area of the PKS biochar increased exponentially, in the order of BC600 (60 min) > BC500 (30 min) > BC500 (90 min) > BC500 (60 min) > BC400 (60 min), with increasing pyrolysis

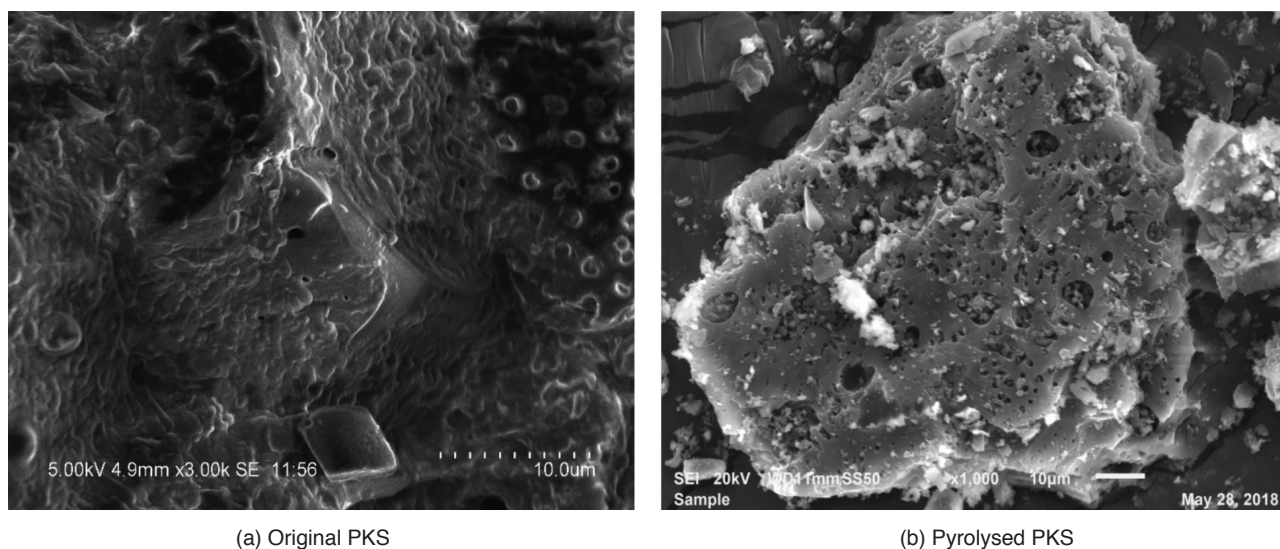


Figure 6. Scanning electron microscope (SEM) monograph of palm kernel shell (PKS). (a) Before pyrolysis (original) and (b) after pyrolysis, BC500 (60 min).

TABLE 1. CHARACTERISTIC FOURIER TRANSFORM INFRARED (FTIR) BANDS OF ORIGINAL AND PYROLYSED PALM KERNEL SHELL (PKS)

Wavenumber (cm <sup>-1</sup> )	3 855	3 737	3 406	2 927	2 850	2 336	1 699	1 579	1 424	1 214	1 055	875	799	536	467
Functional group/bond reference	Monomeric inter- and intramolecular hydrogen bonded (phenolic, water) O-H		Polymeric -OH intramolecular stretching (cellulose)	Aliphatic C-H stretching (cellulose, lignin and hemicellulose)	S-H Stretching, O=C-H <sub>2</sub> , CH <sub>2</sub> asymmetric stretching	Acid O-H stretching	Carbonyl ester C=O stretching	Aromatic C=C stretching	≡C-H bending, =C-H <sub>2</sub> scissoring	Phenolic and ester C-O stretching	Alkoxy C-O and Si-O-Si stretching	Aromatic C-H bending	Aromatic CH out-of-plane	O-H out-of-plane	C-C, S-S stretching
PKS	-	-	3 399	2 923	2 853	2 340	1 720	1 595	1 419	1 238	1 032	875	-	-	-
BC400	3 855	3 748	3 420	2 927	-	2 365	1 705	1 596	1 424	1 168	1 059	875	800	538	464
BC500	3 856	3 742	3 394	-	-	2 323	1 718	1 584	1 424	1 217	1 054	876	800	528	473
BC600	3 869	-	3 409	-	-	2 367	1 703	1 566	1 427	-	1 062	875	-	553	-
BC30	3 852	3 737	3 385	2 929	2 866	-	1 716	1 597	1 424	1 162	1 056	876	796	529	469
BC60	3 856	3 742	3 394	-	-	-	1 718	1 584	1 424	1 217	-	876	-	528	-
BC90	3 859	3 737	3 373	2 927	2 852	-	1 720	1 560	1 424	-	1 056	876	-	537	462

TABLE 2. BRUNAUER EMMET-TELLER (BET) SURFACE AREA, TOTAL PORE VOLUME AND WATER HOLDING CAPACITY OF ORIGINAL AND PYROLYSED PALM KERNEL SHELL (PKS)

Sample	BET surface area (m <sup>2</sup> g <sup>-1</sup> )	Total pore volume (cm <sup>3</sup> g <sup>-1</sup> )	Water holding capacity [g(H <sub>2</sub> O)/10 gl]
PKS	106 ± 3	0.01 ± 0.00	2.23 ± 0.06
BC400 (60 min)	200 ± 9	0.17 ± 0.00	6.07 ± 0.07
BC500 (60 min)	208 ± 9	0.21 ± 0.00	6.11 ± 0.10
BC600 (60 min)	329 ± 4	0.31 ± 0.00	5.87 ± 0.05
BC500 (30 min)	268 ± 3	0.24 ± 0.01	6.21 ± 0.10
BC500 (90 min)	238 ± 2	0.29 ± 0.00	5.26 ± 0.22

temperature while holding time had no effect (Table 2). Recondensed volatile matter that blocked pores gradually evaporated with increasing temperature thus creating new pores and providing additional surface area (Liu *et al.*, 2008; Wannapeera *et al.*, 2008). As shown by SEM monograph (Figure 6), the average measured pore diameter for original PKS was  $0.74 \pm 0.19 \mu\text{m}$  (Figure 6a) while that of BC500 (60 min)  $1.06 \pm 0.22 \mu\text{m}$  (Figure 6b). It is evident that the pore diameter of pyrolysed PKS has increased significantly by at least a factor of 1.4 ( $p < 0.01$ ). However, prolonged pyrolysis at  $>700^\circ\text{C}$  enlarges these pores and finally, they collapse and merge into smaller pores causing structural shrinkage and pore narrowing (Liu *et al.*, 2008).

The water holding capacity increased more than two-fold from its original  $2.23 \text{ g g}^{-1}$  (raw PKS) to a consistent range of  $5.26 - 6.21 \text{ g g}^{-1}$  for PKS biochar produced at different temperatures and holding times. The water holding capacity was in the order of BC500 (30 min)  $>$  BC500 (60 min)  $>$  BC400 (60 min)  $>$  BC600 (60 min)  $>$  BC500 (90 min). As the physical and surface properties of biochar are interrelated, the increase in water holding capacity was attributed to a  $>$ two-fold increase in the surface area and pore volume as discussed. The ability of the produced biochar to hold water is essential for plant growth, especially in sandy soil. In the beginning of thermal processing, the pores of biochar was softened and became more exposed, however, as the biochar was heated further ( $\geq 60$  min), thermal annealing occurred so specific surface area dropped significantly. However, when the pores became larger as in the case of BC600 (60 min) and BC500 (90 min), they could not hold the water as effectively as those of smaller pores. These two PKS biochars held the least amount of water despite possessing the largest total pore volume of  $0.31 \text{ cm}^3 \text{ g}^{-1}$  and  $0.29 \text{ cm}^3 \text{ g}^{-1}$ , respectively. This might be due to an increased hydrophobicity of the surface as a result of a loss of polar functional groups as indicated by low O/C ratios and FTIR spectra.

## CONCLUSION

The water holding capacity of PKS biochar did not vary remarkably with pyrolysis temperature and holding time [BC500 (30 min)  $>$  BC500 (60 min)  $>$  BC400 (60 min)]. The BET surface area was in the order of BC600 (60 min)  $>$  BC500 (30 min)  $>$  BC500 (90 min), while the order of biochar alkalinity was BC600 (60 min)  $>$  BC500 (60 min)  $>$  BC500 (30 min). CEC was in the order of BC400 (60 min)  $>$  BC500 (60 min)  $>$  BC500 (30 min). In terms of CSP, the order was BC500 (90 min)  $>$  BC600 (60 min)  $>$  BC500 (60 min). Valuable plant macronutrients (K, Ca, Mg, P) were retained in PKS biochars produced at  $400$  and  $500^\circ\text{C}$  (BC400 and BC500). From these results

it is concluded that PKS biochar produced at  $500^\circ\text{C}$  and 60 min provides the most promising agronomic and global warming mitigation potential in low fertility, acid soils. At this temperature and holding time, an increased content of carbon coupled with a reduced H and O has thus resulted in a stable biochar with lower H/C and O/C ratios. This together with an increased aromatic C=C functionality further confirm the capability of biochar to sequester carbon for long run. In addition, the beneficial plant macro and micronutrients plus greater water holding capacity of the derived alkaline biochar further add value and enhance any intended soil amendment. However, field trials coupled with a detailed life cycle analysis are required to confirm the projected benefits.

## ACKNOWLEDGEMENT

The authors express their gratitude to the Director-General of MPOB for permission to publish this article. The financial support through the Graduate Students Assistantship (GSAS) Programme is greatly appreciated too. Thank is also due to the technical assistances of the staff from the Energy and Environment Unit, MPOB.

## REFERENCES

- Abdulrazzaq, H; Jol, H; Husni, A and Abu-Bakr, R (2014). Characterization and stabilization of biochars obtained from empty fruit bunch, wood, and rice husk. *Bioresources*, 9(2): 2888-2898.
- Ahmad, M; Moon, D H; Vithanage, M; Koutsospyros, A; Lee, S S; Yang, J E; Lee, S E; Jeon, C and Ok, Y S (2014). Production and use of biochar from buffaloweed (*Ambrosia trifida* L.) for trichloroethylene removal from water. *J. Chem. Technol. Biotechnol.*, 89: 150-157.
- Brewer, C E (2012). *Biochar Characterization and Engineering*. Ph.D thesis, Iowa State University. 197 pp.
- Bridgeman, T G; Jones, J M; Shield, I and Williams, P T (2008). Torrefaction of reed canary grass, wheat straw and willow to enhance solid fuel qualities and combustion properties. *Fuel*, 87(6): 844-856.
- Bridle, T R and Pritchard, D (2004). Energy and nutrient recovery from sewage sludge via pyrolysis. *Water Sci. Technol.*, 50: 169-175.
- Budai, A; Zimmerman, A R; Cowie, A L; Webber, J B W; Singh, B P; Glaser, B; Masiello, C A;

- Andersson, D; Shields, F; Lehmann, J; Camps Arbestain, M; Williams, M; Sohi, S and Joseph, S (2013). Biochar carbon stability test method: An assessment of methods to determine biochar carbon stability. International Biochar Initiative. [https://www.biochar-international.org/wp-content/uploads/2018/04/IBI\\_Report\\_Biochar\\_Stability\\_Test\\_Method\\_Final.pdf](https://www.biochar-international.org/wp-content/uploads/2018/04/IBI_Report_Biochar_Stability_Test_Method_Final.pdf)
- Choi, G-G; Oh, S-J; Lee, S-J and Kim, J-S (2015). Production of bio-based phenolic resin and activated carbon from bio-oil and biochar derived from fast pyrolysis of palm kernel shells. *Bioresour. Technology*, 178: 99-107.
- Clemente, J S; Beauchemin, S; Thibault, Y; Mackinnon, T and Smith, D (2018). Differentiating inorganics in biochars produced at commercial scale using principal component analysis. *ACS Omega*, 3(6): 6931-6944.
- Demirbas, A (2004). Effects of temperature and particle size on bio-char yield from pyrolysis of agricultural residues. *J. Anal. Appl. Pyrol.*, 72(2): 243-248.
- Domingues, R R; Trugilho, P F; Silva, C A; De Melo, I C N A; Melo, L C A; Magriotis, Z M and Sanchez-Monedero, M A (2017). Properties of biochar derived from wood and high-nutrient biomasses with the aim of agronomic and environmental benefits. *PLoS ONE*, 12(5): e0176884.
- Enders, A; Hanley, K; Whitman, T; Joseph, S and Lehmann, J (2012). Characterization of biochars to evaluate recalcitrance and agronomic performance. *Bioresour. Technol.*, 114: 644-653.
- EBC (2012). European biochar certificate - Guidelines for a sustainable production of biochar. European Biochar Foundation (EBC), Arbaz, Switzerland. <http://www.european-biochar.org/en/download>. Version 8E of 1 January 2019. DOI: 10.13140/RG.2.1.4658.7043.
- Gai, X; Wang, H; Liu, J; Zhai, L and Liu, S (2014). Effects of feedstock and pyrolysis temperature on biochar adsorption of ammonium and nitrate. *PLoS ONE*, 9(12): e113888.
- Gaskin, J W; Speir, A; Morris, L M; Ogden, L; Harris, K; Lee, D and Das, K C (2007). Potential for pyrolysis char to affect soil moisture and nutrient status of a loamy sand soil. Working paper in the 2007 Georgia Water Resources Conference, University of Georgia. 27-29 March 2007.
- Galinato, S P; Yoder, J K and Granatstein, D (2011). The economic value of biochar in crop production and carbon sequestration. *Energy Policy*, 39: 6344-6350.
- Haryati, Z; Loh, S K; Kong, S H and Bachmann, R T (2018). Pilot scale biochar production from palm kernel shell (PKS) in a fixed bed allothermal reactor. *J. Oil Palm Res. Vol.* 30(3): 485-494.
- IBI (2015). Standardized product definition and product testing guidelines for biochar that is used in soil. International Biochar Initiative. [https://biochar-international.org/wp-content/uploads/2019/01/IBI\\_Biochar\\_Standards\\_V2.1\\_Final1.pdf](https://biochar-international.org/wp-content/uploads/2019/01/IBI_Biochar_Standards_V2.1_Final1.pdf), accessed on 11 March 2019.
- Imam, T and Capareda, S (2012). Characterization of bio-oil, syn-gas and bio-char from switchgrass pyrolysis at various temperatures. *J. Anal. Appl. Pyrol.*, 93: 170-177.
- Jaafar, A A and Ahmad, M M (2011). Torrefaction of Malaysian palm kernel shell into value-added solid fuels. *Int. J. Chem. Mater. Sci. Eng.*, 5(12): 1-4.
- Jindo, K; Mizumoto, H; Sawada, Y; Sanchez-Monedero, M A and Sonoki, T (2014). Physical and chemical characterization of biochars derived from different agricultural residues. *Biogeosciences*, 11: 6613-6621.
- Karhu, K; Mattila, T; Bergstrom, I and Regina, K (2011). Biochar addition to agricultural soil increased CH<sub>4</sub> uptake and water holding capacity-results from a short-term pilot field study. *Agric. Ecosyst. Environ.*, 140: 309-313.
- Karaosmanoglu, F; Isig-Igur-Ergudenler, A and Sever, A (2000). Biochar from the straw-stalk of rapeseed plant. *Energy Fuels*, 14: 336-339.
- Kim, S W; Koo, B S and Lee, D H (2014). Catalytic pyrolysis of palm kernel shell waste in a fluidized bed. *Bioresour. Technol.*, 167: 425-432.
- Kataki, R; Chutia, R S; Mishra, M; Bordoloi, N; Saikia, R and Bhaskar, T (2015). Feedstock suitability for thermochemical processes. *Recent Advances in Thermochemical Conversion of Biomass* (Ashok Pandey; Bhaskar, T; Stöcker, M and Sukumaran, R K eds.). Elsevier, Amsterdam. p. 31-72.
- Kong, S H; Lam, S S; Yek, P N Y; Liew, R K; Ma, N L; Osman, M S and Wong, C C (2019). Self-purging microwave pyrolysis: An innovative approach to convert oil palm shell into carbon-rich biochar for methylene blue adsorption. *J. Chem. Technol. Biotechnol.*, 94(5): 1397-1405.
- Kong, S H; Loh, S K; Bachmann, R T; Abdul Rahim, S and Salimon, J (2014). Biochar from oil palm biomass: A review of its potential and challenges. *Renew. Sust. Energ. Rev.*, 39: 729-739.

- Krull, E; Baldock, J; Skjemstad, J and Smernik, N (2009). Characteristics of biochar: Organo-chemical properties. *Biochar for Environmental Management: Science and Technology* (Lehmann, J and Joseph, S eds.). London, Earthscan. p. 53-65.
- Li, M F; Li, X; Bian, J; Chen, C Z; Yu, Y T and Sun, R C (2015). Effect of temperature and holding time on bamboo torrefaction. *Biomass Bioenergy*, 83: 366-372.
- Liang, B; Lehmann, J; Solomon, D; Sohi, S; Thies, J E; Skjemstad, J O; Luizao, F J; Engelhard, M H; Neves, E G and Wirrick, S (2008). Stability of biomass derived black carbon in soils. *Geochim. Cosmochim. Acta*, 72: 6069-6078.
- Liu, T F; Fang, Y T and Wang, Y (2008). An experimental investigation into the gasification reactivity of chars prepared at high temperatures. *Fuel*, 87(4-5): 460-466.
- Liu, W-J; Li, W-W; Jiang, H and Yu, H-Q (2017). Fates of chemical elements in biomass during its pyrolysis. *Chemical Reviews*, 117(9): 6367-6398.
- Liu, X; Zhang A; Ji, C; Joseph, S; Bian, R; Li, L; Pan, G and Paz-Ferreiro, J (2013). Biochar's effect on crop productivity and the dependence on experimental conditions - A meta-analysis of literature data. *Plant and Soil*, 373(1): 583-594.
- Loh, S K; Cheong, K Y; Choo, Y M and Salimon, J (2015). Formulation and optimization of spent bleaching earth-based bio organic. *J. Oil Palm Res. Vol.* 27(1): 57-66.
- Loh, S K (2017). The potential of the Malaysian oil palm biomass as a renewable energy source. *Energy Conversion and Management*, 141: 285-298.
- Ma, Z; Yang, Y; Ma, Q; Zhou, H; Luo, X; Liu, X and Wang, S (2017). Evolution of the chemical composition, functional group, pore structure and crystallographic structure of bio-char from palm kernel shell pyrolysis under different temperatures. *J. Anal. Appl. Pyrol.*, 127(38): 350-359.
- Ma, Z; Yang, Y; Wu, Y; Xu, J; Peng, H; Liu, X and Wang, S (2019). In-depth comparison of the physicochemical characteristics of bio-char derived from biomass pseudo components: Hemicellulose, cellulose, and lignin. *J. Anal. Appl. Pyrol.*, 140: 195-204.
- Mahmood, W M F W; Ariffin, M A; Harun, Z; Ishak, N A I M D; Ghani, J A and Rahman, M N A B (2015). Characterisation and potential use of biochar from gasified oil palm wastes. *J. Eng. Sci. Technol. Special Issue on 4<sup>th</sup> International Technical Conference 2014*: 45-54.
- Manickam, T; Cornelissen, G; Bachmann, R T; Ibrahim, I Z; Mulder, J and Hale, S E (2015). Biochar application in Malaysian sandy and acid sulfate soils: Soil amelioration effects and improved crop production over two cropping seasons. *Sustainability*, 7(12): 16756-16770.
- Masek, O; Brownsort, P; Cross, A and Sohi, S (2013). Influence of production conditions on the yield and environmental stability of biochar. *Fuel*, 103: 151-155.
- Mollinedo, J; Schumacher, T E and Chintala, R (2015). Influence of feedstocks and pyrolysis on biochar's capacity to modify soil water retention characteristics. *J. Anal. Appl. Pyrol.*, 114: 100-108.
- Preston, C M and Schmidt, M W I (2006). Black (pyrogenic) carbon in boreal forests: a synthesis of current knowledge and uncertainties. *Biogeosciences*, 3: 211-271.
- Rafiq, M K; Bachmann, R T; Rafiq, M T; Shang, Z; Joseph, S and Long, R (2016). Influence of pyrolysis temperature on physico-chemical properties of corn stover (*Zea mays* L.) biochar and feasibility for carbon capture and energy balance. *PLoS ONE*, 11(6): e0156894.
- Saarnio, S; Heimonen, K and Kettunen, R (2013). Biochar addition indirectly affects N<sub>2</sub>O emissions via soil moisture and plant N uptake. *Soil Biol. Biochem.*, 58: 99-106.
- Shaaban, A; Se, S M; Dimin, M F; Juoi, J M; Mohd Haikal, M H and Mitran, N M M (2014). Influence of heating temperature and holding time on biochars derived from rubber wood sawdust via slow pyrolysis. *J. Anal. Appl. Pyrol.*, 107: 31-39.
- Soda, W; Noble, A D; Suzuki, S; Simmons, R; Sindhusen, L and Bhuthorndharaj, S (2006). Co-composting of acid waste bentonites and their effects on soil properties and crop biomass. *J. Environ. Qual.*, 35: 2293-2301.
- Spokas, K A (2010). Review of the stability of biochar in soils: Predictability of O:C molar ratios. *Carbon Management*, 1(2): 289-303.
- Spokas, K A; Koskinen, W C; Baker, J M and Reicosky, D C (2009). Impact of woodchip biochar additions on greenhouse gas production and sorption/ degradation of two herbicides in a Minnesota soil. *Chemosphere*, 77: 574-581.
- Usman, A R A; Abduljabbar, A; Vithanage, M; Ok, Y S; Ahmad, M; Ahmad, M; Elfaki, J; Abdulazeem, S S

and Al-Wabel, M I (2015). Biochar production from date palm waste: Charring temperature induced changes in composition and surface chemistry. *J. Anal. Appl. Pyrol.*, 115: 392-400.

Uttran, A; Loh, S K; Kong, S H and Bachmann, R T (2018). Adsorption of NPK fertilizers and humic acid on palm kernel shell biochar. *J. Oil Palm Res. Vol. 30(3)*: 472-484.

Van Zwieten, L; Singh, B; Joseph, S; Kimber, S; Cowie, A and Chan, K Y (2009). Biochar and emissions of non-CO<sub>2</sub> greenhouse gases from soil (Ch.13). *Biochar for Environmental Management* (Lehmann, J and Joseph, S eds.). Gateshead, UK, Earthscan. p. 227-249.

Wannapeera, J; Warasuwannarak, N and Pipatmanomai, S (2008). Product yields and

characteristics of rice husk, rice straw and corncob during fast pyrolysis in a drop-tube/fixed-bed reactor. *Songklanakarin J. Sci. Technol.*, 30(3): 393-404.

Yuan, J; Xu, R and Zhang, H (2011). The forms of alkalis in the biochar produced from crop residues at different temperatures. *Bioresour. Technol.*, 102(3): 3488-3497.

Zhang, J; Liu, J and Liu, R (2015). Effect of pyrolysis temperature and heating time on biochar obtained from the pyrolysis of straw and lignosulfonate. *Bioresour. Technol.*, 176: 288-291.

Zheng, H; Wang, Z; Deng, X; Herbert, S and Xing, B (2013). Impacts of adding biochar on nitrogen retention and bioavailability in agricultural soil. *Geoderma*, 206: 32-39.